

Developmental Cell, Volume 25

Supplemental Information

Chromatin Regulation by BAF170 Controls

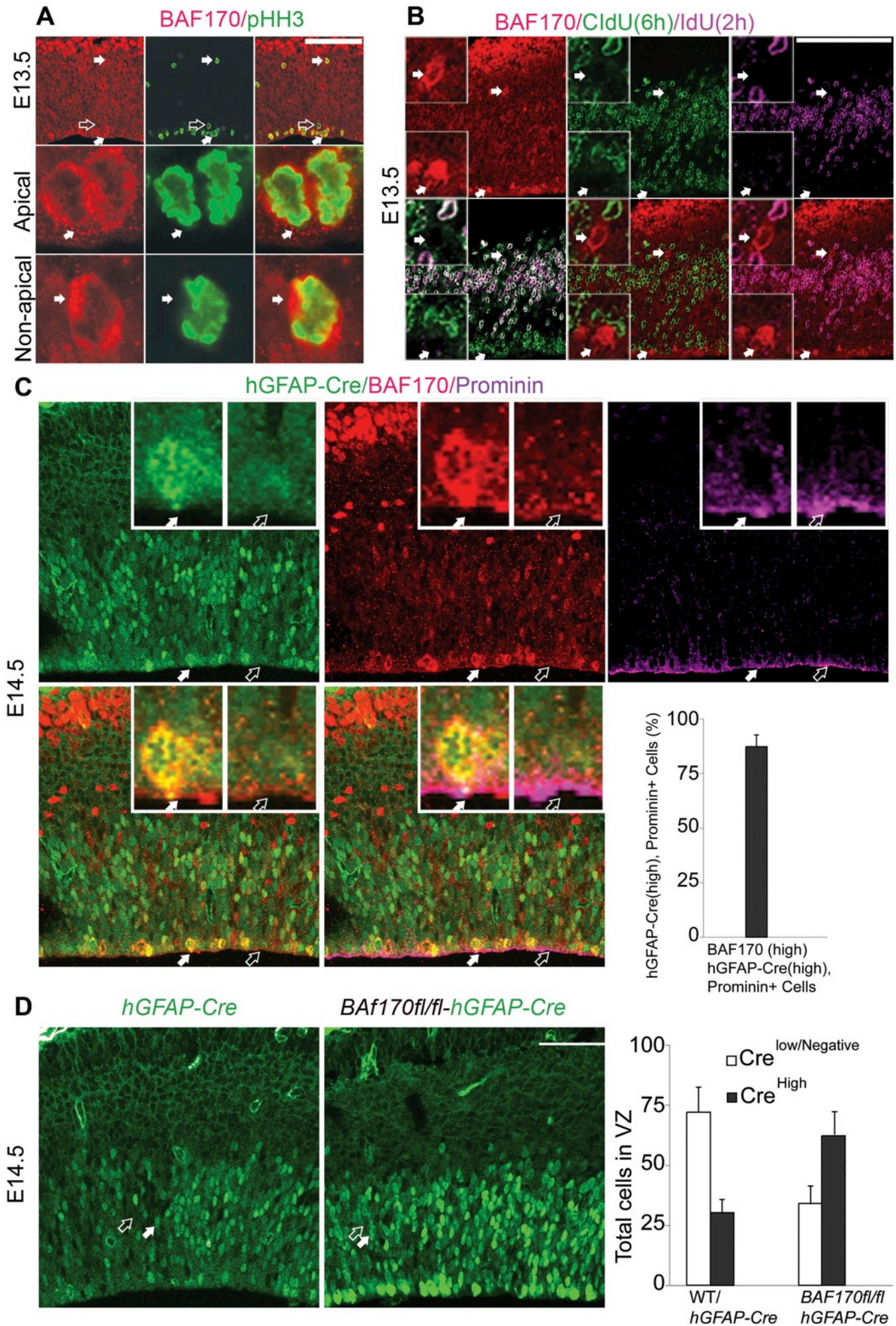
Cerebral Cortical Size and Thickness

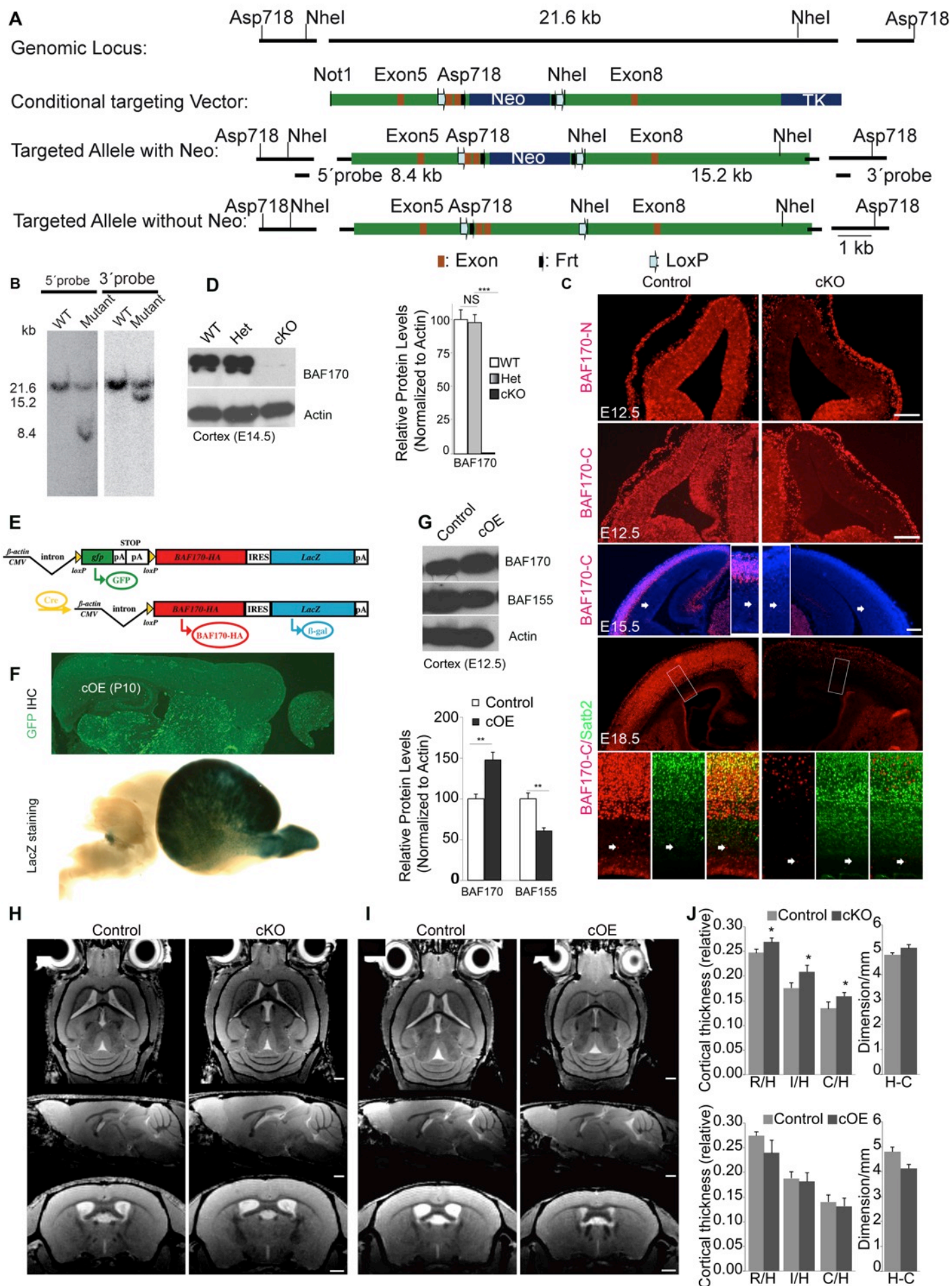
Tran Cong Tuoc, Susann Boretius, Stephen N. Sansom, Mara-Elena Pitulescu, Jens Frahm, Frederick J. Livesey, and Anastassia Stoykova

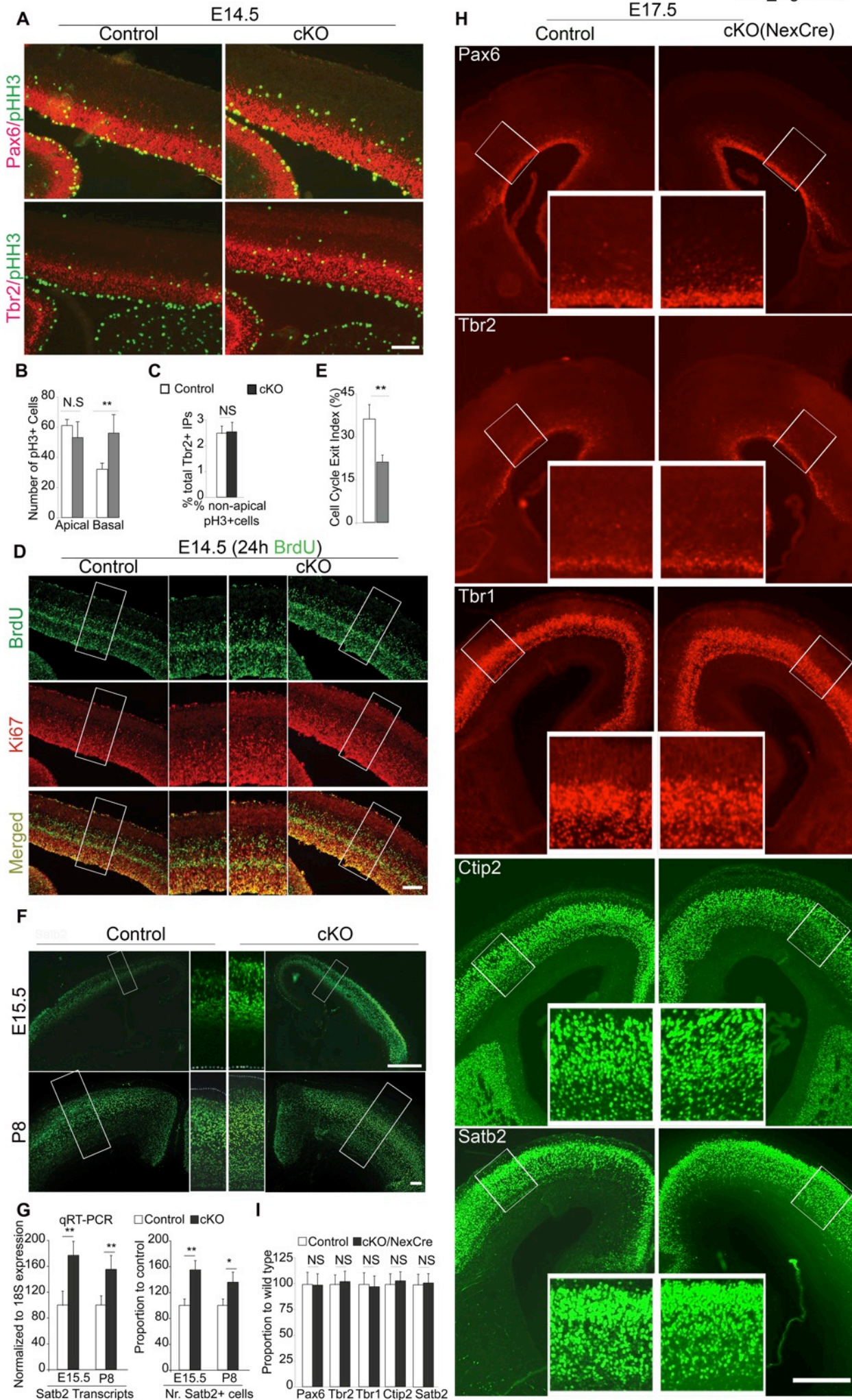
Inventory of Supplementary Materials:

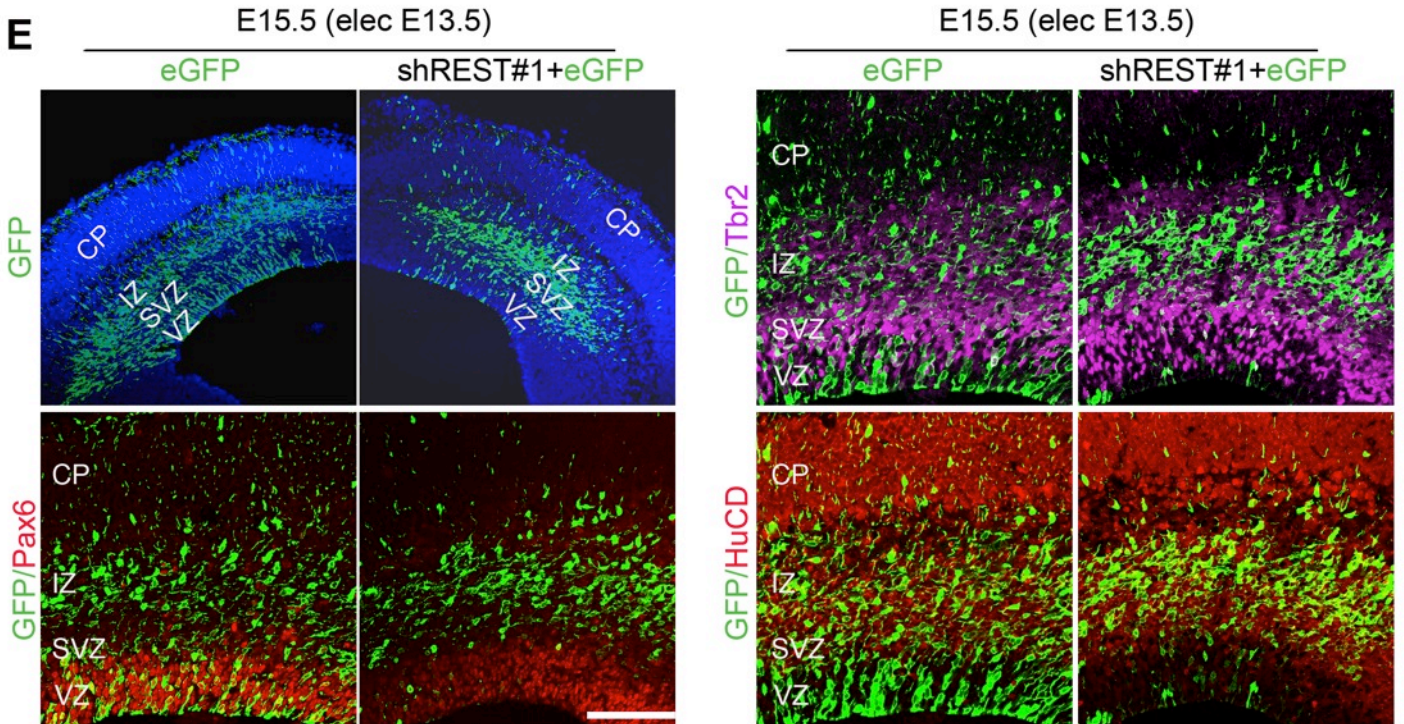
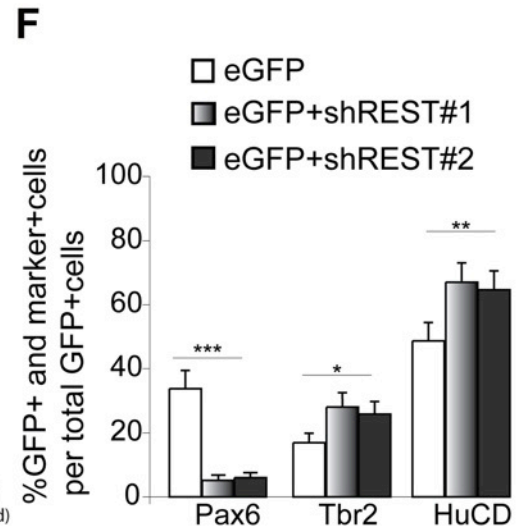
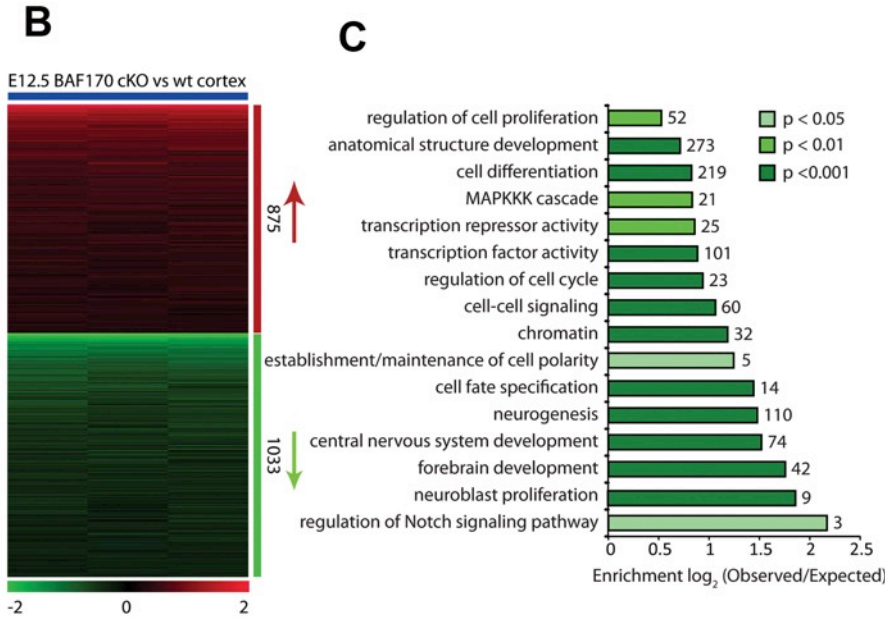
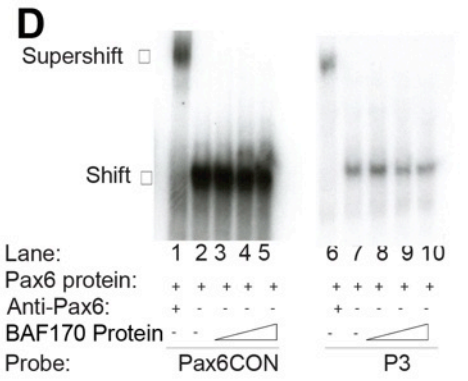
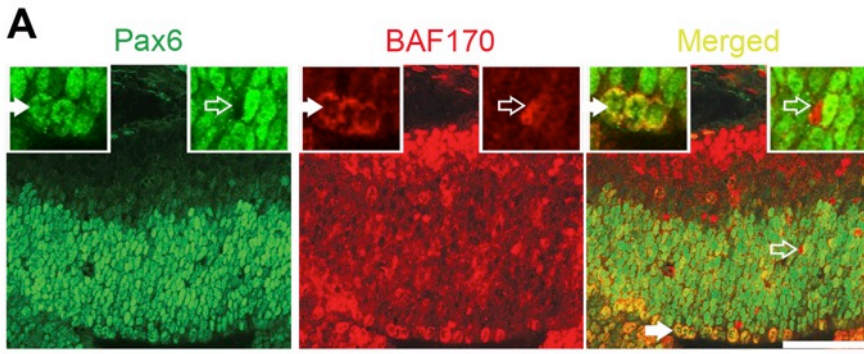
- Figure S1, related to Figure 1: Characterization of BAF170 expression in cortical progenitors.
- Figure S2, related to Figure 2: Generation of transgenic mouse lines for conditional knockout (*BAF170cKO*) or overexpression (*BAF170cOE*) of BAF170 and in vivo MRI measurement of cortical thickness and volume in *BAF170cKO* and *BAF170cOE* mice.
- Figure S3, related to Figure 3: Cell-cycle parameters and deletion of BAF170 in postmitotic neurons.
- Figure S4, related to Figure 3: RGCs daughter fate analysis and neuronal subtype composition of cortical layers in *BAF170cKO* cortex.
- Figure S5, related to Figure 4: Cortical thickness and neuronal density in *BAF170cOE* mice.
- Figure S6, related to Figure 5: Interaction between BAF170 and Pax6 knockdown experiment of REST
- Figure S7, related to Figure 7: Exchange of BAF170 with BAF155 subunits during cortical development.

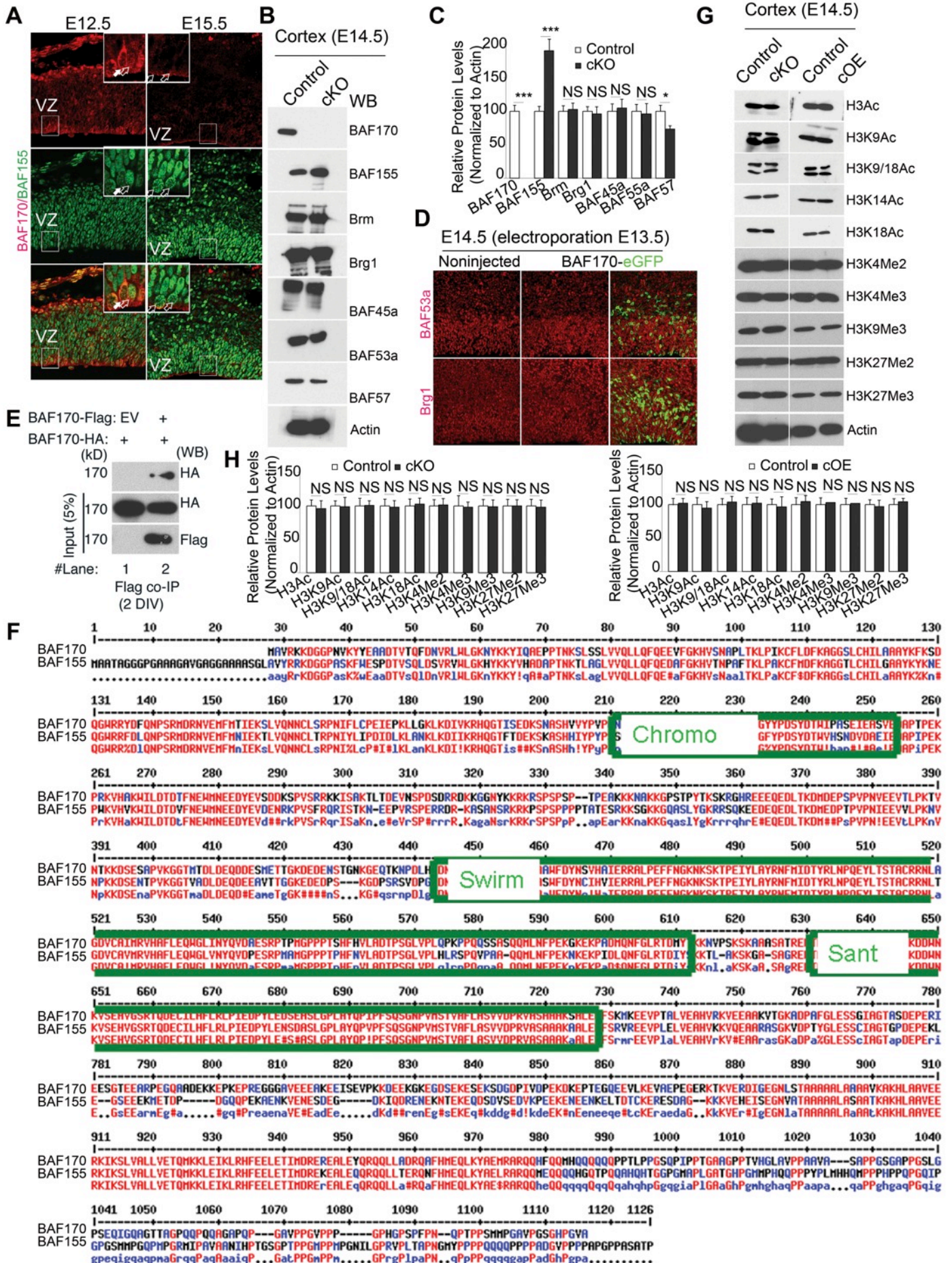
- Table S1, related to figure 5B: Genes regulated by BAF170 in the developing cortex are also regulated by Pax6.
- Supplementary Experimental Procedures
- Supplementary References











SUPPLEMENTAL FIGURE LEGENDS

Figure S1, related to Figure 1.

(A) Images show a double-label IHC analysis with antibodies for BAF170 (red) and pHH3 (green) at E13.5. All mitotic pHH3⁺ cells at the VZ are BAF170-upregulated cells (filled arrows), whereas pHH3⁺ cells, in proximity to the apical surface, are negative for BAF170 (empty arrow).

(B) Triple IHC analysis for BAF170 (red), CidU (green, injected 6 h prior), IdU (magenta, injected 2 h prior) on cross E13.5 brain sections. In overlay images of CidU and IdU, white-labeled cells (CidU⁺/IdU⁺) are in S-phase, whereas green-labeled cells (only CidU⁺) are in G2 phase. The BAF170/CidU and BAF170/IdU labeling pattern indicates that BAF170 is expressed in neither S- nor G2-phase cells.

(C) A triple IHC analysis of brain sections from E14.5 cortices from hGFAP-Cre transgenic mice using antibodies against BAF170 (red), Cre (green), and Prominin (magenta) and statistical analyses reveals that a high proportion of apical RGCs expresses a high level of both BAF170 and Cre (filled arrows). The empty arrows point to RGCs with a low level of expression of both BAF170 and Cre. Thus, during the extensive production of IPs, the strongest BAF170 expression is mostly confined to non-neurogenic RGCs at the apical surface of cortical VZ, in accordance with previously reports (Pinto et al., 2008).

(D) Although loss of *BAF170* function does not affect the total number of RGCs, abrogation of BAF170 leads to a substantial increase in the number of

strongly Cre⁺ non-neurogenic RGP. Images in *inserts* are shown at higher magnification. Scale bars = 250 μm (B), 100 μm (C-D).

Figure S2, related to Figure 2.

(A) Strategy for the generation of transgenic line for conditional *BAF170* knockout (*BAF170cKO*), described in details in the Supplemental Experimental Procedure.

(B) Autography showing a Southern blot analysis of positive ESc clones screened with two (5' and 3') specific external probes.

(C) IHC analysis of E12.5 cortical coronal sections tested with both BAF170-N and BAF170-C antibodies indicates that *BAF170cKO* is a null mutant; the E15.5 and E18.5 cortical sections were tested with the BAF170-C antibody only. Lowest row: Double immunostaining with BAF170 and Satb2 antibodies revealed few BAF170⁺ but Satb2⁻ cells in the lateral cortex of E18.5 *BAF170cKO* brain (white arrows) that most probably represent either migrated from the basal ganglia interneurons and/or descendants of few cortical progenitors that escaped Cre-recombination. Scale bars = 250 μm.

(D) Western blot analysis of protein extracts from cortex of E14.5 control, Heterozygous (Het: *BAF170fl/+;Emx1Cre*) and cKO (*BAF170fl/fl;Emx1Cre*) embryos with BAF170 antibody. Relative levels of BAF170 protein are presented in the diagram to the *right*. The expression of BAF170 is lost in cKO cortices, but still preserved in cortices from BAF170-Het animals as compared with the controls.

(E) Schematic representation of the strategy to generate a transgenic line for conditional overexpression of BAF170 (*BAF170cOE*) described in more details in the Supplemental Experimental Procedure.

(F) After crossing *BAF170cOE* with the *Emx1Cre* line, the majority of cortical cells in the double-transgenic animals were GFP-negative (successful recombination), while subcortical regions (where no recombination occurs) strongly expressed GFP. Whole-mount of double transgenic brains stained for β -galactosidase indicate specific expression of the LacZ-reporter in the cortex and olfactory bulb, and a lack of expression in the mesencephalon, and diencephalons.

(G) Protein levels of BAF170, BAF155 were examined by Western blotting of tissue samples from *BAF170cOE* and control cortices at E12.5. Relative levels of BAF170 and BAF155 protein are presented in the diagram below the blot. Values are presented as means \pm SEMs (*P < 0.05; **P < 0.01; ***P < 0.005; n = 4, cortical tissues from 4 control and 4 cOE mice of two different founders).

(H-I) Horizontally (top), sagittally (middle) and axially (bottom) oriented MT-weighted images of a control and a cKO mouse (H), a control and a cOE mouse (I), resolution: 100 x 100 x 100 μm^3 , Scale bars = 1 mm.

(J) Upper Left diagram: Cortical thickness relative to the dorsoventral dimension of the brain (H) measured on lines perpendicular to the corpus callosum in rostral (R), intermediate (I) and caudal (C) brain regions (see also

Figure 2). The diagram on the right represents the brain dorsoventral height excluding the cortex (H-C) in *BAF170cKO*.

The lower diagrams represents the corresponding cortical parameters in the *BAF170cOE* mutant. * significant with $p < 0.0125$ chosen as level of significance adjusted for 4 variables tested

Figure S3, related to Figure 3.

(A) Images show double IHC for RGC marker Pax6 and phosphorylated histone H3 (pHH3), a marker for mitotically active cells and double IHC for Tbr2/pHH3.

(B) Statistical analysis indicated that, although the loss of BAF170 had no effect on the number of pHH3⁺ cells at the apical cortical surface, it did lead to nearly a 2-fold increase in the number of pHH3⁺ cells in the basal surface of the VZ where IPs are located.

(C) Although loss of *BAF170* function causes a substantial increase in the number of Tbr2+IPs and non-apical pHH3 cells, however, the ratio of the number of non-apical pHH3⁺ cells and Tbr2+IPs is not affected. For (A-C) counting was done on pictures, including entire sections.

(D) *cKO* and control embryos were injected at E13.5 with BrdU for 24 h. Images show double-label IHC of BrdU and Ki67 (a marker for progenitors in all except for G2 phase of the cycle) at E14.5.

(E) Statistical analysis revealed that the cell-cycle-exit index (number of BrdU⁺/Ki67⁻ cells per total number of BrdU⁺ cells) was significantly lower in

BAF170cKO than in control cortices. The counting was done in frames (300 μ m x 650 μ m) of digitalized pictures.

Values are expressed as means \pm SEMs (n = 4). Scale bars = 250 μ m.

(F) Images show IHC analysis with an anti-Satb2 antibody at the indicated stages.

(G) Statistical analysis indicated that both Satb2 expression level estimated through qRT-PCR (left diagram) and the Satb2⁺ cell density were increased in *BAF170cKO* mice compared to controls. The counting was done in frames (100 μ m x 300 μ m for E15.5; 200 μ m x 600 μ m for P8) of digitalized pictures.

(H) Immunostaining of coronal sections of E17.5 brains with specific antibodies for RGCs (Pax6), IPs (Tbr2), early-born neurons (Ctip2, Tbr1), and late-born neurons (Satb2), and histograms (in I) from statistical comparisons showed no evident variations in the number of immunopositive cells in *BAF170cKO_NexCre* mice and control cortices. The counting was done in frames (200 μ m x 250 μ m) of digitalized pictures. Values are expressed as means \pm SEMs (*P < 0.05; **P < 0.01; ***P < 0.005; n = 4). Scale bars = 500 μ m.

Figure S4, related to Figure 3.

(A) E13.5 brains of same *BAF170fl/fl* littermates were electroporated with either pCIG2-Cre-ires-eGFP (Cre-eGFP) or pCIG2-ires-eGFP (eGFP). After 24 h paired sections of isolated brains are examined for eGFP expression (in green). Note that in the control (eGFP) brain, GFP⁺ cells show a wider

distribution above the ventricular zone as compared to the experimental brain (Cre-eGFP).

(B) Tripple IHC GFP (green), Tuj1 (red) and Tbr2 (magenta) antibodies reveals a preferable generation of Tbr2⁺IPs in the Cre-eGFP injected brain (B3, B4, C). Cre-eGFP-electroporated cortices contained only rarely GFP⁺/Tuj1⁺ neurons (0.5%) as compared with eGFP-treated control cortices (18±2.5%) (filled arrows). (B1, B2, C) The number of GFP⁺/Tbr2⁺ cells (with a fate of Ips, empty arrows) was significantly increased in Cre-eGFP-injected cortices (57±6%) as compared with the Cre-eGFP-treated control cortex (32±4%). The arrowheads point to GFP⁺/Tuj1⁺/Tbr2⁺ cells, representing advanced in their differentiation IPs (Arai et al., 2011; Englund et al., 2005). The lower panels show selected frames (1, 2, 3) at higher magnification of GFP⁺/Tuj⁺/Tbr2⁻ cells (1), GFP⁺/Tuj⁻/Tbr2⁺ cells (2), GFP⁺/Tuj⁺/Tbr2⁺ cells (3). The statistical analysis of the data is shown in (C).

(D, E) Cortical LLs and ULs are illustrated by IHC with Tbr1 antibody on matched *BAF170cKO* and control brains sagittal (D, left) and coronal (D, right) sections at P8. In (E) are shown higher magnification pictures of the fields (boxed in D) in which measurements for thicknesses of Tbr1+LLs and ULs were done. On matched sagittal sections these include rostral (R, motor), and caudal (C) cortex; in coronal sections: dorsal (D, motor) and lateral (L, somatosensory) cortex. The counting (E/F) was done in frames (300 µm x 900 µm) of digitalized pictures in fields shown in (D). The frame (SS) indicates the selected field used for cell counting after staining of P8 and P10 brain sections for different markers as stated in the text.

(F) Statistical analyses comparing the thickness of LLs and ULs (marked by Tbr1 expression, as shown in E) in control and *BAF170cKO* cortices. Note that *BAF170cKO* exhibits increased thickness compared to the control in the entire cortex, but prominently in the UL.

(G) IHC with TAG1 antibody revealed in corpus callosum (CC) of *BAF170cKO* animals an enhanced interhemispheric axonal projection pattern as compared with the controls, confirmed also by increase in the relative intensity of the TAG1 fluorescent signal (shown in the diagram below the panel). The arrows point to expanded lateral CC wings in the mutant brain and abundance of corticofugal axons in capsula interna (pointed in frames).

(H) IHC analyses of *BAF170cKO* cortices at E14.5 and *BAF170cOE* cortices at E15.5 with an anti-Casp-3 antibody (red) indicates that loss- and gain-of-*BAF170* function does not cause apoptosis. Values are presented as means \pm SEMs (*P < 0.05; **P < 0.01; ***P < 0.005; n = 4). Scale bars = 250 μ m (D) and 100 μ m (E).

Figure S5, related to Figure 4.

(A-B) Cortical LLs and ULs on sagittal P10 brain sections from control and *BAF170cOE* animals are outlined by the expression of Tbr1 at two levels, lateral (a, a') and medial (b, b'). The frames in rostral (R) and caudal (C) cortex point the fields in which measurement for thicknesses of Tbr1+LLs and ULs were performed on matched sections. Panels B and C illustrate the immunostaining patterns and statistical evaluation of LL and UL thickness in control and *BAF170cOE* cortices, respectively. Note that the thickness of the

entire cortex is decreased in *BAF170cOE* compared to the control, but the ULs are more severely affected. The counting (B/C) was done in digitalized frames (300 μm x 900 μm) of pictures in fields shown in (A).

(D) Statistical comparison of the density of L6 neurons in *BAF170cOE* and control cortices, as indicated by the expression of specific markers. Values are presented as means \pm SEMs (n = 4). Scale bars = 250 μm .

Figure S6, related to figure 5.

(A) Double-label IHC analysis with anti-BAF170 (red) and anti-Pax6 (green) antibodies indicate that BAF170 and Pax6 are co-expressed in radial glial progenitors and apical surface pHH3⁺ cells (filled arrow), but not in non-apical surface pHH3⁺ cells (empty arrow). Images in inserts are shown at higher magnification. Scale bars = 250 μm .

(B) Microarray analysis of gene expression changes in the cortex of *BAF170cKO* mice at E12.5. Gene expression was quantified in three wild-type and three *BAF170cKO* cortices on six single-color Illumina BeadChip microarrays. Ratios of wild-type and *BAF170cKO* pairs are clustered to show the 875 up-regulated and 1033 down-regulated genes identified (Benjamini-Hochberg corrected p-value < 0.05).

(C) Selected Gene Ontology categories enriched in the set of genes with significant changes in expression in the *BAF170cKO* cortex. Significantly enriched categories were identified by comparison with the complete set of genes represented by the microarray using a Benjamini & Hochberg corrected Hypergeometric test.

(D) EMSA (electromobility band shift assay) was performed using purified Pax6 and BAF170 proteins, and Pax6-binding consensus probes P6CON and P3. Note that Pax6 binding to P6CON and P3 was unaltered by increasing amounts of BAF170 protein.

(E, left panel) E13.5 brains were electroporated with either shREST(#1, #2) plasmids *plus* GFP plasmid or GFP plasmid alone. Two days after electroporation (E15.5), matching sections were examined for the location of GFP+cells. In GFP-injected cortices, a large population of GFP+cells migrated into IZ and CP, while many GFP+cells were still in VZ/SVZ. However, in GFP *plus* shREST-injected cortices, most GFP+cells were in SVZ and region above SVZ/IZ whereas only very few GFP+cells were kept in VZ.

(E, right panel). Double IHC analyses were performed to examine the co-expression of GFP and Pax6 (RGCs), Tbr2 (IPs), HuC/D (neurons) and the quantitative results are presented in (F). Note that cortices electroporated with GFP *plus* shREST plasmids contained much less GFP+/Pax6+RGCs ($5.2 \pm 0.7\%$ with shREST#1 and $6.1 \pm 0.8\%$ with shREST#2) compared to that of GFP-treated controls ($34 \pm 4.7\%$). In contrast, the number of GFP+/Tbr2+positive cells was significantly increased in GFP *plus* shREST-injected brains ($28.1 \pm 3.2\%$ with shREST#1 and $25.2 \pm 3.5\%$ with shREST#2) as compared to GFP-treated cortices ($17.5 \pm 0.28\%$). The number of GFP+/HuCD+ neurons in GFP *plus* shREST-injected cortices ($67 \pm 4.9\%$ with shREST#1 and $65 \pm 5.1\%$ with shREST#2) was greater than that in GFP alone-injected cortices ($49 \pm 4.7\%$) (E-F). These data indicate that *REST* play

important role in different aspects of cortical development, including the genesis of IPs.

Figure S7, related to figure 7.

(A) Double immunostaining of cross E12.5 and E15.5 sections with anti-BAF170 (red) and anti-BAF155 (green) antibodies under the same confocal imaging conditions shows a dynamic of the expression of these two BAF subunits in the cortical progenitors. Note that while at E12.5 a moderate expression of both subunits was detected, after the almost complete abolishment of the expression of BAF170 in cortical progenitors at E15.5, the expression of BAF155 in the progenitors showed a strong up-regulation.

(B-D) The expression of distinct npBAF subunits was examined by both Western blotting of samples from *BAF170*cKO cortices (B,C) and by IHC on cortices electroporated with BAF170-eGFP plasmid (D) with antibodies as indicated. Relative levels of indicated BAF subunits are presented in the diagram (C). Values are presented as means \pm SEMs (*P < 0.05; **P < 0.01; ***P < 0.005; n = 3, cortical tissues from 3 control and 3 cKO mice. Note that alteration of BAF170 expression affected the expression of BAF155 and BAF57. The expression of most other subunits (i.e., Brm, Brg, BAF45a, BAF53a) was normal following alteration of BAF170 expression. Scale bars = 250 μ m.

(E) BAF170 protein is capable of forming dimers. Primary cortical progenitors from E12.5 embryos were electroporated with HA-tagged BAF170 (BAF170-HA) and FLAG-tagged BAF170 (BAF170-Flag). After 2 DIV, the interaction of

BAF170-HA and BAF170-Flag was demonstrated by Flag co-immunoprecipitation, indicating that one BAF complex in cortical progenitors might contain at least two molecules of BAF170.

(F) Alignment of amino acid sequences for BAF170 and BAF155 proteins.

(G-H) Expression of modified H3 was evaluated in tissues from E14.5 *BAF170*cKO and *BAF170*cOE cortices by Western blotting (F). In (G) the relative levels of modified histones (H3) are presented in the diagrams. Values are presented as means \pm SEMs (*P < 0.05; **P < 0.01; ***P < 0.005; n = 3, cortical tissues from 3 control, 3 cOE and 3 cKO mice). Note that although *BAF170*LOF and GOF affected DNA methylation, and repressive and active chromatin marks at the loci of some *Pax6*-target promoters (see Figure 7D-F) the overall level of the examined H3 modifications was unchanged with loss or over-expression of BAF170.

Table. Sequences of qRT-PCR, ChIP and genotyping primers, EMSA probes, and shRNA.

Oligo name	Sequence, Source
qPax6/F	CCTGGTTGGTATCCCGGGA
qPax6/R	CCGCTTCAGCTGAAGTCGCA
qTuj	QT00124733 (Qiagen)
qCTIP2	QT01061809 (Qiagen)

qCux2	(Sessa et al., 2008)
qSvet1	(Sessa et al., 2008)
qLmo4	(Sessa et al., 2008)
qNeuroD1	(Sessa et al., 2008)
qCux1	QT00168910 (Qiagen)
qTle1	QT00172991 (Qiagen)
qSatb2	QT00142394 (Qiagen)
qBhlhb5	QT00266924 (Qiagen)
qBLBP	QT00109865 (Qiagen)
qGLAST	QT00146223 (Qiagen)
q18S	QT01036875 (Qiagen)
qGapdh	QT00309099 (Qiagen)
Pax6CON	Tuoc & Stoykova, 2008
P3	Tuoc & Stoykova, 2008
TO515	GATGCCTGCTTGCCGAATATCATG
TO516	CATGGTGGCTCTCCTAAGCAATCCAA
TO517	CTGGCTTTGTGTGTGTGTGTTTGTTTC

shREST#1	Jorgensen et al., 2009
shREST#2	Jorgensen et al., 2009

Table S1, related to Figure 5 (as a separate file).

Genes regulated by BAF170 in the developing cortex are also regulated by Pax6 (A and B). Genes significantly up (A) or down (B) regulated in the cortex of three E12.5 BAF170 cKO embryos in comparison to three wild-type littermate controls. (C) Selected Gene Ontology categories significantly enriched among *BAF170* regulated genes. (D) Genes regulated by both BAF170 and Pax6 in the E12.5 neocortex. (E) Selected genes regulated by BAF170 and Pax6 that are known to be important for cortical development. Details of these analyses are provided in the tables and Methods.

SUPPLEMENTAL EXPERIMENTAL PROCEDURES

Plasmids

Plasmids used in this study (and their origins): Pax6 (mouse Pax6 cDNA in pBDLeu, Invitrogen); CMV-Pax6 (mouse Pax6 cDNA in pCMV), Flag-Pax6 (mouse Pax6 cDNA in pCS2-MT); pCAX-Pax6 (mouse Pax6 cDNA in pCAX, a gift from Dr. Noriko Osumi, Tohoku University); shPax6#1-2 (target sequences for mouse BAF170 in the oligo list; from OriGene); BAF170 (mouse BAF170 in pPC86, Invitrogen), BAF170-Flag (human BAF170 in pCMV-Flag, from Addgene); BAF170-HA-ires-GFP (mouse BAF170 cDNA in

pCIG2, a gift from Dr Francois Guillemot, NIMR London); shBAF170#1-4 (target sequences for mouse BAF170 in the oligo list; from SABiosciences); Brm-Flag (human Brm in pCMV-Flag, Brm cDNA from Addgene); pCON/P3 (2xP6CON plus 3xP3 sequences in pGL3 basic, Promega as (Tuoc and Stoykova, 2008); pTbr2 (a gift from Dr. Miyata, Nagoya University); pCux1 (containing 1.1 kb of *Cux1* promoter in pGL3 basic, Promega); pTle1 (containing 0.8 kb of *Tle1* promoter in pGL3 basic, Promega). REST (mouse REST cDNA in pCS2-MT, a gift from Dr Anderson, California Institute of Technology); shRESTs (Jorgensen et al., 2009); pSRG3-Luc (containing BAF155 promoter, (Jang et al., 2006); Truncated Flag-BAF170s (Peng et al., 2009)

Antibodies

Polyclonal (pAb) and monoclonal (mAb) antibodies used in this study (working dilution; sources): Pax6 mAb (1:200; DSHB), Pax6 rabbit pAb (1:500 for WB and 1:200 for IHC; BABCO), β -actin rabbit pAb (1:1000; Sigma), Flag mAb (1:1000; Sigma), BAF170 rabbit pAb (1:100; Cat. IHC-00213, Bethyl, or BAF170-C which is raised against an epitope as peptide at C-terminal of BAF170), BAF170 rabbit pAb (1:100; Cat. NB100-92393, Novus Biologicals or BAF170-N which is raised against an epitope as peptide at N-terminal of BAF170), BAF170 rabbit pAb (1:100; Cat. HPA021213), BAF170 rabbit pAb (Cat. A301-038A), BAF170 goat pAb (Cat. sc-9744, Santa Cruz), BAF45a, BAF45c, BAF53a, BAF53b rabbit pAb (gift from Dr Crabtree, Stanford University), BAF57 rabbit pAb (Bethyl), BAF155 rabbit pAb (Santa Cruz), BAF155 mouse mAb (Santa Cruz), Brg1 rabbit pAb (Santa Cruz), Brg1 mouse mAb (Santa Cruz), Brm mouse mAb (BD Biosciences), Brm rabbit pAb

(Abcam), phospho-H3 mAb (1:50; Cell Signaling), phospho-Vimentin mAb (1:500; MBL), Tbr2 rabbit pAb (1:300; Chemicon), Tuj mAb (1:200; Chemicon), Tbr1 rabbit pAb (1:300; Chemicon), Ctip2 rat pAb (1:200; Abcam), FoxP2 rabbit pAb (1:500; Abcam), BLBP rabbit pAb (1:200; Millipore), RC2 mouse mAb (1:50; DSHB), GLAST guinea pig pAb (1:100; Millipore), β -catenin mAb (1:100; BD Pharmingen), BrdU mouse mAb (1:40; CalTag), BrdU rat pAb (1:100; Abcam), Ki67 rabbit pAb (1:50; Vector Laboratories), Satb2 mouse mAb (1:100; Abcam), Casp-3 rabbit pAb (1:100; Cell Signaling), GFP rabbit pAb (1:1000; Abcam), GFP chick pAb (1:1000; Abcam), Er81 rabbit pAb (1:1000; a gift from Dr. Silvia Arber, University of Basel), RORc mouse mAb (1:100; Perseus Proteomics), Cux1 rabbit pAb (1:100; Santa Cruz), Tle4 rabbit pAb (1:100; Abcam), Bhlhb5 goat pAb (1:50; Santa Cruz), Brn2 goat pAb (1:200; Santa Cruz), Tle1 rabbit pAb (1:200; Abcam), Brm rabbit pAb (ChIP; Abcam), Brg1 rabbit pAb (ChIP; Santa Cruz), REST rabbit pAb (ChIP; Millipore), REST mouse mAb (1: 200, a gift from Dr Anderson, California Institute of Technology), H3K9me3 rabbit pAb (Abcam), H3K27me2 rabbit pAb (Cell Signaling), H3Ac rabbit pAb (Upstate), H3K9Ac rabbit pAb (Abcam), H3K27me3 rabbit pAb (Upstate), H3K4me2 rabbit pAb (Cell Signaling), H3K4me3 rabbit pAb (Cell Signaling), H3K9/18Ac rabbit pAb (upstate, 2000), H3K14Ac rabbit pAb (Upstate), H3K18Ac rabbit pAb (Abcam), Sin3A rabbit pAb (ChIP; Millipore), MeP2 rabbit pAb (ChIP; Abcam), HDAC rabbit pAb (ChIP; Abcam), peroxidase-conjugated goat anti-rabbit IgG (1:10000; Covance), peroxidase-conjugated goat anti-mouse IgG (1:5000; Covance), peroxidase-conjugated goat anti-rat IgG (1:10000; Covance), Alexa 488, Alexa 568, Alexa 594, Alexa 647 (1:400; Molecular Probes).

Animals

A detailed description of the generation of *BAF170^{fl/fl}* and *BAF170cOE* mice is provided in below sections. *BAF170^{fl/fl}*, *BAF170cOE*, *Small-eye* mutant (allele *Sey*) (Hill et al., 1991), *floxed Pax6* (Ashery-Padan et al., 2000), *Emx1-Cre* (Gorski et al., 2002), *hGFAP-Cre* (Zhuo et al., 2001), *Nex-Cre* (Goebbels et al., 2006), *CMV-Cre* (Schwenk et al., 1995) mice were maintained in a C57BL6/J background. In majority of the experiments, we used *Emx1-Cre* line to generate cortex-specific *BAF170cKO* mice (referred as cKO) or cortex-specific overexpressing *BAF170cOE* (referred as cOE) mice. In some studies, *hGFAP-Cre*, *Nex-Cre* and *CMV-Cre* were used to generate *BAF170cKO_hGFAP*, *BAF170cKO_Nex*, *BAF170cKO_CMV*, respectively, as indicated in the text. Animals were handled in accordance with the German Animal Protection Law and with the permission of the Bezirksregierung Braunschweig.

Generation of *BAF170^{fl/fl}* mice

The conditional gene-targeting vector was constructed using a recombineering approach as described previously (Liu et al., 2003) and shown schematically in Figure S1. RPCI-21 Mouse 129s6/SvEvTAC (F) PAC Library (BACPAC Resources Center) was screened with a *BAF170* genomic probe to identify a BAC clone containing the *BAF170* genomic locus. A gap-repair plasmid was generated by two-step cloning to retrieve the plasmid (5' arm, *NotI/SpeI*; 3' arm, *SpeI/XbaI*; 200–500-bp in length) in pL253 (Liu et al.,

2003). A 22-kb fragment from the screened clone was then retrieved into the PL253 ESC targeting vector (Liu et al., 2003). Two LoxP sites plus an Frt-flanked *Neo* cassette (outside of exons 6 and 7) were targeted to the resulting construct in two steps in EL350 cells through recombineering (Liu et al., 2003). First, to insert the single 5' loxP site, a targeting cassette containing P_{gk}-em7-neo flanked by homology arms to regions 5' of *BAF170* exon 6 was constructed in the PL400 plasmid. The targeting cassette was released through co-electroporation into heat-shock-induced EL350 cells, as described previously (Liu et al., 2003). The P_{gk}-em7-neo sequence was then removed by electroporation into arabinose-induced, Cre-expressing EL350 cells, leaving behind a single loxP site. The second loxP site 3' of *BAF170* exon 7 was inserted by first constructing a targeting cassette containing frt-P_{gk}-Em7-neo-frt-loxP in the PL451 plasmid. The conditional targeting vector was then linearized by *NotI* digestion and electroporated into 129-derived CJ7 ESCs using standard procedures. G418 (180 µg/ml) and ganciclovir (2 µM) double-resistant clones were analyzed by Southern-blot hybridization using both 5' and 3' external probes (Figure S1). Correctly targeted clones were then injected into C57BL/6 blastocysts using standard procedures, and the resulting chimeras were mated with C57BL/6 females to obtain germline transmission of the targeted (*Neo*) allele. The conditional knockout (cKO) allele was obtained by crossing *BAF170*^{neo} mice to β-actin-Flp transgenic mice. The KO allele eliminates exons 6 and 7 in *BAF170* which encode the CHROMO (Chromatin organization modifier) domain, and shifts the open reading frame of the subsequent sequence. *BAF170*^{fl/fl} mice were maintained

by back-crossing heterozygous mice to control C57BL/6 mice. These *BAF170^{fl/fl}* mice were viable and fertile with no apparent abnormalities.

Mice were genotyped by a PCR-based method using tail DNA. This genotyping procedure used three sets of primers (TO515, TO516, TO517; sequences are presented in the primer table) that amplify 327-bp (control allele), 780-bp (floxed allele), and 473-bp (Flr allele) fragments. PCR cycling conditions were as follows: 95°C for 5 minutes; 32 cycles of 95°C for 30 seconds, 58°C for 40 seconds, and 72°C for 50 seconds; 72°C for 10 minutes; and hold at 4°C.

Generation of *BAF170*cKO mice

To ablate the function of *BAF170* during early cortical neurogenesis, we used the *Emx1Cre* line as a driver for recombinase activity (Gorski et al., 2002). We crossed *BAF170^{fl/+};Emx1Cre^{+/+}* with *BAF170^{fl/fl}* mice, which progeny showed the following genotypes: 25% of *BAF170^{fl/fl};Emx1Cre^{+/+}* (cKO), 25% of *BAF170^{fl/+};Emx1Cre* (Het), 25% of *BAF170^{fl/fl}*, and 25% of *BAF170^{fl/+}*. The cortical size (as described below) of *BAF170^{fl/+};Emx1Cre^{+/+}* (Het) and *BAF170^{fl/fl}* mice was not altered and used as controls. To study the effect of *BAF170* ablation in postmitotic neurons of cortical plate, we used the *NexCre* line (Goebbels et al., 2006). *BAF170^{fl/+};NexCre^{+/+}* mice were crossed to *BAF170^{fl/fl}* mice and brain sections from mutant (*BAF170^{fl/fl};NexCre^{+/+}*) and control (*BAF170^{fl/fl}*) brains were analyzed by IHC as described in the text. To generate *BAF170* full KO we used the ubiquitous delete *CMV-Cre* mouse line (Schwenk et al., 1995).

Generation of *BAF170cOE* mice

BAF170cDNA together with a HA tag sequence was cloned into *pJO* plasmid (Berger et al., 2007). The cDNA construct (*pJO-BAF170*) was used to generate *via* pronuclear microinjection mice (*CMV/βactin-loxP-GFPpolyA-loxP-BAF170-HA-IRES-LacZ*) allowing expression of transgenic BAF170 upon recombination (see also Figure S2E, F, G).

To overexpress *BAF170* in the early cortical progenitors (*BAF170cOE*), the generated transgenic female mice (*pJo-BAF170*) were crossed with the males of *Emx1Cre* line (Gorski et al., 2001) to produce double transgenic *BAF170cOE* brains (*LacZ+/Emx1Cre+*) and controls (either *LacZ-/Emx1Cre+* or *LacZ+/Emx1Cre* –negative brains).

Quantitative analysis of immunohistochemical signal intensity

For the quantitative analyses of immunohistochemical signal intensity of BAF170, Cre (Figure S1C/D), *Tbr2*, *Cux1*, *Tle1* (Figure 5D), the confocal fluorescent images were analyzed with ImageJ (software freeware) with Line Analyzer function to measure pixel values of selected cells as previously described (Tuoc and Stoykova, 2008). This approach allowed us to subdivide the BAF170+cells and Cre+ cells in VZ into different subpopulations, highly expressing BAF170 or highly expressing Cre (*BAF170^{high}* or *Cre^{high}*, intensity of fluorescent signals >30 pixels), and with a low /or negligible BAF170 or low /or negligible Cre staining (*BAF170^{low}* or *Cre^{low}*, intensity of fluorescent signals <30 pixels).

For the quantitative analyses of immunohistochemical signal intensity of TAG1 (Figure S4G), fluorescent images of entire sections of forebrains at both

rostral and caudal levels were used. The color images of forebrains were converted to gray scale to eliminate background. The pixel values of fluorescent signals intensity were measured by using Analyze/Analyze Particles function (ImageJ software).

mRNA Expression profiling and data analysis

Probes passing a detection p-value threshold of 0.01 were selected using the R package lumi (Du et al., 2008). The data were then transformed using variance stabilisation (Lin et al., 2008) and quantile normalised before the identification of significant changes in gene expression (eBayes, Benjamini-Hochberg corrected p-value < 0.05) using Limma (Smyth, 2005). Before the comparison all microarray probes were re-annotated to the latest MGI gene symbols using ProbeLynx (<http://koch.pathogenomics.ca/probelynx/>), (Roche et al., 2004), and genes not to both common microarray platforms were removed from the analysis. Significant changes in gene expression in the E12.5 *BAF170cKO* cortex were clustered using the MeV software (Saeed et al., 2003) and Gene Ontology analysis was performed using GOToolBox (<http://genome.crg.es/GOToolBox/>), (Martin et al., 2004)). Intersection probabilities were calculated using a hypergeometric test as previously described (Fury et al., 2006).

Cortical progenitor culture and reporter assays

Cortical progenitors were dissociated from E12.5 mice and cultured as described previously (Conti et al., 2005; Tuoc and Stoykova, 2008). For reporter assays, plasmids were transfected into NIH3T3 cells using

Lipofectamine 2000 or electroporated into cultured cortical progenitors using a Mouse NSC Nucleofector Kit and a nucleotransfection device (Amaxa). Luciferase assays were performed as described previously (Tuoc and Stoykova, 2008). For drug treatments, 100 nM TSA (Calbiochem) or 100 nM 5-aza-dC (Sigma) were added to cultured cortical progenitors, and treated cells were cultured in Sato medium for an additional 1 or 2 days, as described previously (Tuoc and Stoykova, 2008).

Protein-protein interaction assay

Yeast analysis and Flag IP were performed as described previously (Tuoc and Stoykova, 2008).

Western blot analysis and protein quantification

Western blot analysis was performed as described previously (Tuoc and Stoykova, 2008). The relative amount of Pax6 protein was quantified densitometrically using ImageJ software.

***In vivo* co-IP of BAF170 and Pax6 and Flag IP**

Cortical regions from E13.5 mice were dissected in ice-cold 1.3 M sucrose tissue cracking buffer (TC buffer; 10 mM HEPES pH 7.6, 25 mM KCl, 1 mM EDTA pH 8.0, 10% glycerol (v/v), 1.3 M sucrose, 1 mM dithiothreitol [DTT], 1 mM phenylmethanesulfonylfluoride or phenylmethylsulfonyl fluoride [PMSF], protease inhibitor cocktail)(Lessard et al., 2007). The tissues were Dounce-homogenized and the sucrose concentration was adjusted to 1.5 M with a 2 M sucrose TC buffer. The homogenate was layered over a cushion of TC buffer containing 2 M sucrose, and the nuclei were pelleted by ultracentrifugation at

30,000 rpm for 1 hour at 4°C. After removing the lipid layers, the nuclear pellet was washed three times with nuclear buffer 3 (10 mM HEPES pH 7.6, 100 mM KCl, 0.1 mM EDTA pH 8.0, 10% glycerol (v/v), 3 mM MgCl₂, 1 mM DTT, 1 mM PMSF, protease inhibitor cocktail). In addition, nuclear extracts were treated for 30 min at room temperature with DNase/benzonase (20 U/reaction). After the final wash, the nuclear pellet was resuspended in 500 µl nuclear buffer 3 and Dounce-homogenized. The homogenate was incubated on ice for 30 minutes, collected by centrifugation, and Dounce homogenized a second time.

Goat polyclonal anti-BAF170 (C-19) antibody (Santa Cruz) or rabbit polyclonal Pax6 (BABCO) or corresponding negative control (goat IgG, rabbit IgG) were incubated with immobilized Protein G beads and cross-linked with disuccinimidyl suberate (DSS; Pierce). Protein G-bound antibodies (7.5 µg) were incubated overnight at 4°C with 450 µg E13.5 cortical nuclear extract in binding/wash buffer (140 mM NaCl, 8 mM sodium phosphate, 2 mM potassium phosphate and 10 mM KCl, pH 7.4) with gentle rotation. The beads were washed seven times with 500 µl binding/wash buffer, and then complexes were eluted with 100 µl ImmunoPure IgG elution buffer (pH 2.8) and neutralized with 1 M Tris-Cl pH 9.5. Samples were boiled with SDS loading buffer for 5 minutes, and 8% of input and 20% of IP elute were resolved by SDS-PAGE on 8% gels for Western blot analysis with an anti-Pax6 antibody.

Flag IP were performed as described (Tuoc and Stoykova, 2008) with small modification. Cell extracts were treated for 30 min at room temperature with DNase/benzonase (10 U/reaction) before addition of Flag beads.

Electrophoretic mobility shift assay (EMSA)

EMSA was performed as described previously (Tuoc and Stoykova, 2008) with some modifications. Briefly, HeLa cells were transiently transfected with mammalian expression constructs for either Flag-Pax6 or Flag-BAF170 using Lipofectamine 2000. Forty-eight hours later, cells were harvested and exogenously expressed proteins were purified using Anti-Flag M2 Affinity Gel (Sigma). The purified proteins – 50 ng of purified Pax6 proteins and increasing amounts (50, 100, and 150 ng) of purified BAF170 proteins – were combined in binding reactions.

ChIP analysis

For ChIP analyses, cortical progenitors were prepared from control, *BAF170*cKO and *Sey/Sey* mice and cultured as described previously (Conti et al., 2005). ChIP experiments were performed using an EZ ChIP assay kit (Millipore), according to the supplier's instructions. Antibodies were used as indicated in the list of antibodies. A genomic fragment of the *Trim11* gene and a GFP antibody plus IgG were used as negative DNA and antibody controls, respectively (Tuoc and Stoykova, 2008).

Bisulfite genomic analysis

Genomic DNA from cortices of *BAF170*cKO, control or *in utero* electroporated mice was treated with sodium bisulfite to convert all unmethylated cytosine residues into uracil residues by using EpiTect Bisulfite kit (Qiagen), according to the supplier's instructions. Different genomic DNA fragments were amplified

and cloned into pGEM-T vector. Twenty-four clones were randomly picked from three independent bisulfite treatments and PCR amplifications. The cloned plasmids were examined by sequencing. Sequences of picked clones were further selected and analyzed by using BiQ Analyzer software (Bock et al., 2005)

qRT-PCR

qRT-PCR analyses were performed as described previously (Tuoc and Stoykova, 2008) using primers described in below table.

REFERENCES

Arai, Y., Pulvers, J.N., Haffner, C., Schilling, B., Nusslein, I., Calegari, F., and Huttner, W.B. (2011). Neural stem and progenitor cells shorten S-phase on commitment to neuron production. *Nat Commun* 2, 154.

Berger, J., Berger, S., Tuoc, T.C., D'Amelio, M., Cecconi, F., Gorski, J.A., Jones, K.R., Gruss, P., and Stoykova, A. (2007). Conditional activation of Pax6 in the developing cortex of transgenic mice causes progenitor apoptosis. *Development* 134, 1311-1322.

Bishop, K.M., Garel, S., Nakagawa, Y., Rubenstein, J.L., and O'Leary, D.D. (2003). Emx1 and Emx2 cooperate to regulate cortical size, lamination, neuronal differentiation, development of cortical efferents, and thalamocortical pathfinding. *The Journal of comparative neurology* 457, 345-360.

Bishop, K.M., Rubenstein, J.L., and O'Leary, D.D. (2002). Distinct actions of Emx1, Emx2, and Pax6 in regulating the specification of areas in the developing neocortex. *The Journal of neuroscience : the official journal of the Society for Neuroscience* 22, 7627-7638.

Bock, C., Reither, S., Mikeska, T., Paulsen, M., Walter, J., and Lengauer, T. (2005). BiQ Analyzer: visualization and quality control for DNA methylation data from bisulfite sequencing. *Bioinformatics* 21, 4067-4068.

Conti, L., Pollard, S.M., Gorba, T., Reitano, E., Toselli, M., Biella, G., Sun, Y., Sanzone, S., Ying, Q.L., Cattaneo, E., *et al.* (2005). Niche-independent symmetrical self-renewal of a mammalian tissue stem cell. *PLoS Biol* 3, e283.

Du, P., Kibbe, W.A., and Lin, S.M. (2008). lumi: a pipeline for processing Illumina microarray. *Bioinformatics* 24, 1547-1548.

Englund, C., Fink, A., Lau, C., Pham, D., Daza, R.A., Bulfone, A., Kowalczyk, T., and Hevner, R.F. (2005). Pax6, Tbr2, and Tbr1 are expressed sequentially by radial glia, intermediate progenitor cells, and postmitotic neurons in developing neocortex. *J Neurosci* 25, 247-251.

Fury, W., Batliwalla, F., Gregersen, P.K., and Li, W. (2006). Overlapping probabilities of top ranking gene lists, hypergeometric distribution, and stringency of gene selection criterion. Conference proceedings : Annual International Conference of the IEEE Engineering in Medicine and Biology Society IEEE Engineering in Medicine and Biology Society Conference 1, 5531-5534.

Goebbels, S., Bormuth, I., Bode, U., Hermanson, O., Schwab, M.H., and Nave, K.A. (2006). Genetic targeting of principal neurons in neocortex and hippocampus of NEX-Cre mice. *Genesis* 44, 611-621.

Gorski, J.A., Talley, T., Qiu, M., Puelles, L., Rubenstein, J.L., and Jones, K.R. (2002). Cortical excitatory neurons and glia, but not GABAergic neurons, are produced in the Emx1-expressing lineage. *J Neurosci* 22, 6309-6314.

Jang, J., Choi, Y.I., Choi, J., Lee, K.Y., Chung, H., Jeon, S.H., and Seong, R.H. (2006). Notch1 confers thymocytes a resistance to GC-induced apoptosis through Deltex1 by blocking the recruitment of p300 to the SRG3 promoter. *Cell death and differentiation* 13, 1495-1505.

Jorgensen, H.F., Terry, A., Beretta, C., Pereira, C.F., Leleu, M., Chen, Z.F., Kelly, C., Merckenschlager, M., and Fisher, A.G. (2009). REST selectively represses a subset of RE1-containing neuronal genes in mouse embryonic stem cells. *Development* 136, 715-721.

Lessard, J., Wu, J.I., Ranish, J.A., Wan, M., Winslow, M.M., Staahl, B.T., Wu, H., Aebersold, R., Graef, I.A., and Crabtree, G.R. (2007). An essential switch in subunit composition of a chromatin remodeling complex during neural development. *Neuron* 55, 201-215.

Lin, S.M., Du, P., Huber, W., and Kibbe, W.A. (2008). Model-based variance-stabilizing transformation for Illumina microarray data. *Nucleic acids research* 36, e11.

Liu, P., Jenkins, N.A., and Copeland, N.G. (2003). A highly efficient recombineering-based method for generating conditional knockout mutations. *Genome Res* 13, 476-484.

Martin, D., Brun, C., Remy, E., Mouren, P., Thieffry, D., and Jacq, B. (2004). GOToolBox: functional analysis of gene datasets based on Gene Ontology. *Genome biology* 5, R101.

Peng, G., Yim, E.K., Dai, H., Jackson, A.P., Burgt, I., Pan, M.R., Hu, R., Li, K., and Lin, S.Y. (2009). BRIT1/MCPH1 links chromatin remodelling to DNA damage response. *Nat Cell Biol* 11, 865-872.

Pinto, L., Mader, M.T., Irmeler, M., Gentilini, M., Santoni, F., Drechsel, D., Blum, R., Stahl, R., Bulfone, A., Malatesta, P., *et al.* (2008). Prospective isolation of functionally distinct radial glial subtypes--lineage and transcriptome analysis. *Mol Cell Neurosci* 38, 15-42.

Roche, F.M., Hokamp, K., Acab, M., Babiuk, L.A., Hancock, R.E., and Brinkman, F.S. (2004). ProbeLynx: a tool for updating the association of microarray probes to genes. *Nucleic acids research* 32, W471-474.

Saeed, A.I., Sharov, V., White, J., Li, J., Liang, W., Bhagabati, N., Braisted, J., Klapa, M., Currier, T., Thiagarajan, M., *et al.* (2003). TM4: a free, open-source system for microarray data management and analysis. *BioTechniques* 34, 374-378.

Sahara, S., and O'Leary, D.D. (2009). Fgf10 regulates transition period of cortical stem cell differentiation to radial glia controlling generation of neurons and basal progenitors. *Neuron* 63, 48-62.

Sansom, S.N., Griffiths, D.S., Faedo, A., Kleinjan, D.J., Ruan, Y., Smith, J., van Heyningen, V., Rubenstein, J.L., and Livesey, F.J. (2009). The level of the transcription factor Pax6 is essential for controlling the balance between neural stem cell self-renewal and neurogenesis. *PLoS Genet* 5, e1000511.

Schwenk, F., Baron, U., and Rajewsky, K. (1995). A cre-transgenic mouse strain for the ubiquitous deletion of loxP-flanked gene segments including deletion in germ cells. *Nucleic Acids Res* 23, 5080-5081.

Smyth, G. (2005). Limma: Linear models for microarray data. *Bioinformatics and Computational Biology Solutions using R and Bioconductor*. Springer, New York, 397-420.

Tuoc, T.C., and Stoykova, A. (2008). Trim11 modulates the function of neurogenic transcription factor Pax6 through ubiquitin-proteasome system. *Genes Dev* 22, 1972-1986.